

Dissipation-Driven Phase Transition in Two-Dimensional Josephson Arrays

Luca Capriotti,^{1,2} Alessandro Cuccoli,^{3,4} Andrea Fubini,^{3,5} Valerio Tognetti,^{3,4,6} and Ruggero Vaia^{7,4}

¹Valuation Risk Group, Credit Suisse First Boston (Europe) Ltd., One Cabot Square, London E14 4QJ, United Kingdom

²Kavli Institute for Theoretical Physics, University of California, Santa Barbara, California 93106, USA

³Dipartimento di Fisica dell'Università di Firenze - via G. Sansone 1, I-50019 Sesto Fiorentino (FI), Italy

⁴Istituto Nazionale per la Fisica della Materia - U.d.R. Firenze - via G. Sansone 1, I-50019 Sesto Fiorentino (FI), Italy

⁵MATIS-INFM and DMFCI, Università di Catania, viale A. Doria 6, I-95125 Catania, Italy

⁶Istituto Nazionale di Fisica Nucleare, Sezione di Firenze, via G. Sansone 1, I-50019 Sesto Fiorentino (FI), Italy

⁷Istituto dei Sistemi Complessi del Consiglio Nazionale delle Ricerche, Sezione di Firenze, via Madonna del Piano, I-50019 Sesto Fiorentino (FI), Italy

(Received 14 October 2004; published 21 April 2005)

We analyze the interplay of dissipative and quantum effects in the proximity of a quantum phase transition. The prototypical system is a resistively shunted two-dimensional Josephson junction array, studied by means of an advanced Fourier path-integral Monte Carlo algorithm. The reentrant superconducting-to-normal phase transition driven by quantum fluctuations, recently discovered in the limit of infinite shunt resistance, persists for moderate dissipation strength but disappears in the limit of small resistance. For large quantum coupling our numerical results show that, beyond a critical dissipation strength, the superconducting phase is always stabilized at sufficiently low temperature. Our phase diagram explains recent experimental findings.

DOI: 10.1103/PhysRevLett.94.157001

PACS numbers: 74.81.Fa, 02.70.Uu, 03.65.Yz, 03.75.Lm

Dissipation due to coupling with the surrounding environment [1] is an unavoidable effect accompanying the operation of any microscopic or mesoscopic quantum device. The knowledge of the influence of dissipative effects on quantum coherence and quantum phase transitions (QPT) is therefore essential to assess the reliability of such devices in performing tasks which strongly depend on the possibility to maintain entanglement (phase coherence), e.g., in quantum computation. Among the quantum devices that have already found wide application, many are based on a collection of regularly arranged or single small Josephson junctions [2,3]. These are also among the candidates for the physical implementation of the so-called *qubits* [4].

Josephson junction arrays (JJA), are prototypical systems displaying a quantum phase transition with a control parameter tuning the strength of quantum fluctuations. This has become progressively clear after it was pointed out [5] in the late 1970s that the charging energy of Josephson-coupled superconducting grains could lead to the quenching of the collective superconducting phase. Since then, several studies [2,3] have been devoted to characterizing the superconductor-normal (SN) transition in JJA. Among the systems studied, the two-dimensional (2D) ones are the most interesting as no true long-range order is possible at finite temperature while a genuine QPT occurs at $T = 0$ [6]; moreover, 2D samples can be fabricated in a controlled way and experimentally characterized [7–9].

The main effect of dissipation in JJA is that of quenching the quantum fluctuations of the phase variables (thereby enhancing those of the conjugate charges) thus stabilizing the S phase [10–16]. This has had ingenious experimental

confirmations, e.g., in a JJA coupled with a 2D electron gas substrate that allows one to tune the dissipation strength [8], as well as in identical JJA with different built-in Cr shunt resistors [9].

In this Letter we use a Fourier path-integral Monte Carlo (PIMC) approach to analyze the competition between dissipation and quantum fluctuations in JJA, for strong quantum coupling and in proximity of the QPT. In particular, we study the phase diagram as a function of temperature, quantum coupling, and dissipation. We show how a large enough dissipation leads to the disappearance of the zero-temperature QPT, as well as of the reentrant low-temperature behavior displayed in the limit of large shunt resistance [17]. The phase diagram we obtain is in remarkable agreement with the experimental one. Concerning the reentrance, we can explain the two distinct behaviors found in experiments; indeed, a nonmonotonic (i.e., reentrant) low-temperature behavior of the array resistance has been observed in unshunted JJA [7], but not in shunted ones [9].

JJA are essentially described by the quantum XY model, whose coordinates and momenta correspond to the wavefunction phases $\hat{\varphi}_i$ and the net Cooper-pair number (charge) \hat{n}_i , respectively, of superconducting islands arranged on a lattice

$$\hat{\mathcal{H}} = \frac{(2e)^2}{2} \sum_{ij} C_{ij}^{-1} \hat{n}_i \hat{n}_j - \frac{E_J}{2} \sum_{i\mathbf{d}} \cos(\hat{\varphi}_i - \hat{\varphi}_{i+\mathbf{d}}), \quad (1)$$

where $[\hat{\varphi}_i, \hat{n}_j] = i\delta_{ij}$ and \mathbf{d} runs over the z nearest-neighbor displacements. The Josephson energy E_J sets the energy scale, making it convenient to use the dimensionless temperature $t = T/E_J$, while the charging energy involves the capacitance matrix $C_{ij} = C\Gamma_{ij}^{(\eta)}$, with

$\Gamma_{ij}^{(\eta)} = (z\delta_{ij} - \sum_d \delta_{i,j+d}) + \eta\delta_{ij}$, including the mutual capacitance C and the self-capacitance $C_0 \equiv \eta C$; in the experimental samples C is typically dominant [7,9], i.e., $\eta \ll 1$. We consider here a square lattice, $z = 4$.

In the classical limit (large C) the charging term is thermodynamically irrelevant and the SN transition is a Berezinskii-Kosterlitz-Thouless (BKT) one [18], leading from a high- T disordered phase to a low- T quasicrystalline phase at $t_c = 0.892$ [19]. The S phase is weakened [3] by the quantum fluctuations of the phase when the characteristic charging energy $E_C = (2e)^2/2C$ is comparable to the Josephson energy E_J , i.e., when the quantum coupling constant $g = \sqrt{E_C/E_J}$ is of the order of unity [20]. The coupling parameter g can be varied in the fabrication of JJA, and its further increase can finally drive the zero- T system through a QPT at a critical value g_c , numerically [21] estimated ≈ 3.4 . Near the QPT the system is characterized by a sharp enhancement of anharmonic quantum fluctuations [17].

In this Letter we consider normal Ohmic shunt resistors R_S as the source of dissipation, whose strength is measured by the dimensionless parameter $\gamma = R_Q/R_S$, with the resistance quantum $R_Q = h/(2e)^2$. It is well known that dissipation enhances the S phase, i.e., $t_c(g, \gamma)$ increases with γ , but reliable results could be obtained only in the low-coupling regime [10,20]. Mean field, renormalization group, and variational approaches [12–15] predict the existence of a critical value $\gamma_c = 2/z = 1/2$ above which the QPT disappears and for any value of g the system is in the S phase at sufficiently low temperature. Moreover, it is not clear whether the reentrant behavior (with the N phase reappearing at lower T) observed at $\gamma = 0$ in the proximity of g_c [17] disappears before or at the critical value γ_c . As these phenomena involve the strong coupling region where approximate theories give contradictory answers [22], accurate numerical data are required for a real understanding, as well as for the interpretation of the experimental data.

To this purpose we employ an efficient Fourier PIMC technique recently introduced [17,23]. This starts from the path integral for the effective partition function $Z = \int \mathcal{D}\varphi \exp\{-S[\varphi] - S_I[\varphi]\}$, where the action $S[\varphi]$ corresponds to the Hamiltonian (1) and $S_I[\varphi]$ is the bilocal influence action [1,13,24], namely,

$$S[\varphi] = \int_0^{1/t} du \left[\sum_{ij} \frac{\Gamma_{ij}^{(\eta)}}{4g^2} \dot{\varphi}_i(u) \dot{\varphi}_j(u) - \frac{1}{2} \sum_{id} \cos \varphi_{id}(u) \right], \quad (2)$$

$$S_I[\varphi] = \frac{1}{2} \int_0^{1/t} du du' \kappa(u-u') \sum_{id} [\varphi_{id}(u) - \varphi_{id}(u')]^2. \quad (3)$$

Here $u \in [0, 1/t]$ is the (dimensionless) “imaginary time”, $\varphi_{id} = \varphi_i - \varphi_{i+d}$, and $\kappa(u) = \gamma t^2/8 \sin^2(\pi t u)$ is the dissipative Ohmic kernel. The strongly nonlocal dependence of the kernel on $u - u'$ can be easier dealt with in

the (time) Fourier space (with the Matsubara frequencies $\omega_k \equiv 2\pi k t$ and k integer), as the influence action turns into a local form [13,24], namely, $S_I[\varphi] = \frac{\gamma}{4} \sum_{id} \sum_k |k| |\varphi_{idk}|^2$, suggesting that dissipation can be easier dealt with in this way. Therefore, at variance with the standard PIMC algorithm, that samples the variables $\{\varphi_{i\ell} = \varphi_i(\ell/Pt), \ell = 1, \dots, P\}$ after discretization of the interval $u \in [0, 1/t]$ in P slices of size $1/Pt$ (P being the Trotter number), we proposed [23] to sample the P Fourier components of $\varphi_{i\ell}$. Choosing $P = 2M + 1$ one can write

$$\varphi_{i\ell} = \bar{\varphi}_i + 2 \sum_{k=1}^M \left(\varphi_{ik}^{(R)} \cos \frac{2\pi \ell k}{P} + \varphi_{ik}^{(I)} \sin \frac{2\pi \ell k}{P} \right). \quad (4)$$

The $2M$ components $\{\varphi_{ik}^{(R)}, \varphi_{ik}^{(I)}\}$ and the zero-frequency component $\bar{\varphi}_i$ are sampled by the Metropolis algorithm. Monte Carlo autocorrelation times can be significantly reduced by alternating Metropolis moves with microcanonical over-relaxed ones [17,25]. However, the real improvement in simulation efficiency arises from the fact that the move amplitudes can be independently chosen and dynamically adjusted for each Fourier component, thus correctly sampling also strongly fluctuating paths [23,26]. Eventually, the finite- P overall action $S + S_I$ reads

$$\sum_{ij} \sum_{k=1}^M T_{ijk} \left(\varphi_{ik}^{(R)} \varphi_{jk}^{(R)} + \varphi_{ik}^{(I)} \varphi_{jk}^{(I)} \right) - \frac{1}{2Pt} \sum_{id} \sum_{\ell=1}^M \cos \varphi_{id\ell}, \quad (5)$$

where the “kinetic” matrix $T_{ijk} = \frac{P^2 t}{g^2} \sin^2 \frac{\pi k}{P} \Gamma_{ij}^{(\eta)} + \gamma k \Gamma_{ij}^{(0)}$ and the Josephson interaction term is to be expressed using the expansion (4): note that it does not burden the simulation as the $\{\varphi_{i\ell}\}$ are stored and just updated in the component to be moved, at variance with the integral appearing in standard Fourier PIMC algorithms [27]. We performed an extensive set of simulations involving $L \times L$ square lattices

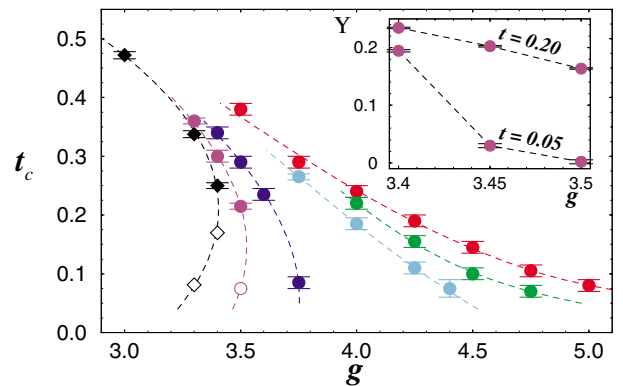


FIG. 1 (color online). Phase diagram for the square-lattice JJA with $\eta = 0.01$ for increasing values of the dissipation strength $\gamma = R_Q/R_S = 0$ (diamonds), 0.15, 0.25, 0.4, 0.45, and 0.5 (circles, from left to right). Inset: Trotter- and size-extrapolated helicity modulus $Y(g, t)$ for $\gamma = 0.15$, at $t = 0.2$ and $t = 0.05$.

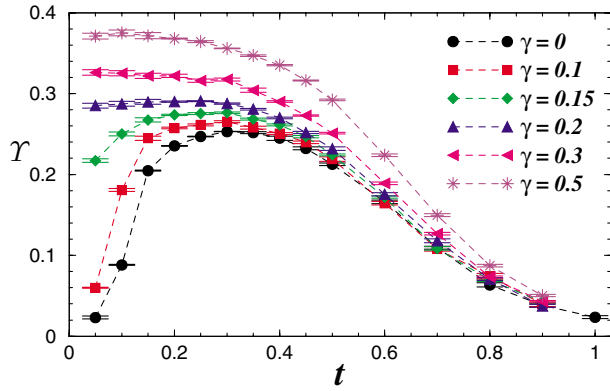


FIG. 2 (color online). Temperature behavior of the helicity modulus $Y(t)$, on the 8×8 lattice and $P \rightarrow \infty$, for $g = 3.4$ and different dissipation strengths, showing that with rising γ the reentrant behavior disappears and $Y(t)$ becomes monotonic for $\gamma \gtrsim 0.2$.

ces with linear sizes up to $L = 48$ and Trotter numbers up to $P = 201$, setting $\eta = 0.01$.

Our main results concern the phase diagram in the (t, g) plane for different values of the dissipation strength γ , and are summarized in Fig. 1; the data points were obtained for $P = 101$ as in Ref. [17] by fitting the finite-size scaling relation for the helicity modulus (or stiffness) per island $Y = (L^2 E_J)^{-1} [\partial^2 F / \partial q^2]_{q=0}$, defined as the response of the free energy $F(q)$ under twisting the boundary conditions as $\varphi_i \rightarrow \varphi_i + \mathbf{q} \cdot \mathbf{i}$.

As shown in Fig. 1, in addition to generally stabilizing the S phase, dissipation hinders the mechanism causing the reentrance. However, the reentrance persists for small values of γ and only a finite value $\gamma \gtrsim 0.2$ restores a monotonic critical line. The persistence of a reentrant normal phase for $\gamma = 0.15$ is illustrated in the inset of Fig. 1, where the thermodynamic helicity modulus, as obtained through a systematic finite-size scaling analysis, is plotted as a function of the quantum coupling: at $g = 3.5$ it appears that Y keeps a finite value for $t = 0.20$, while it vanishes for $t = 0.05$, thus signaling that the established phase coherence disappears again at low temperature.

It is interesting to see how the temperature behavior of $Y(t)$ changes with γ in the region of the reentrance. In Fig. 2 several finite-lattice data for $g = 3.4$ show that rising γ removes the reentrance to disorder at low temperature, as if g were decreased [17]. From these data one can again roughly estimate that the threshold where the reentrance disappears is at $\gamma \simeq 0.2$.

Further increasing γ , the critical line in Fig. 1 progressively changes its curvature and an inflexion point appears for $\gamma \gtrsim 0.4$, signaling the incipient stabilization of a low-temperature S phase for any value of the quantum coupling, as we argue below. In order to address this important issue, we study the dependence on γ of the helicity modulus and related quantities at higher values of g , namely $g = 5$ and $g = 10$, and at a fixed low temperature $t = 0.05$. In Fig. 3 we report the helicity modulus and the “pure-

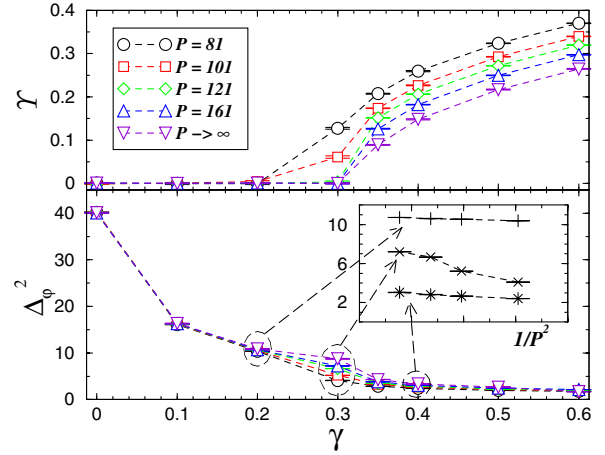


FIG. 3 (color online). Finite-size data ($L = 24$) for Y (top panel) and Δ_φ^2 (bottom panel) vs γ , at $t = 0.05$ and $g = 5$, for different values of P . Inset: $1/P^2$ extrapolation of Δ_φ^2 .

quantum” spread of the phase difference between neighboring islands [17,28], namely $\Delta_\varphi^2 = \langle [\varphi_{id}(u) - \varphi_{id}]^2 \rangle$, for $g = 5$ and different Trotter numbers including the extrapolation to $P \rightarrow \infty$. For increasing dissipation, Y remains zero in an interval and then, around a crossover value $\gamma \simeq 0.3$, it abruptly starts to increase; for slightly larger γ the critical curve $t_c(g, \gamma)$ is hence expected to cross the point $(g = 5, t = 0.05)$. The crossover is clearly connected with the quenching of the pure-quantum phase fluctuations (lower panel of Fig. 3). Just at the crossover, the PIMC data for Δ_φ^2 display the phenomenon of a markedly weaker convergence with P (see inset), signaling that fluctuations of high Matsubara modes become significant: this may reflect the proximity to a phase transition mainly driven by quantum fluctuations, which are in turn modulated by the dissipation.

Since at $g = 5$ the system displays a BKT transition for $\gamma \gtrsim 0.3$, a much larger coupling is required to check whether $\gamma \geq \gamma_c = 1/2$ in fact ensures low- t ordering. We therefore performed simulations for quantum coupling as large as $g = 10$, as reported in Fig. 4. Again a crossover

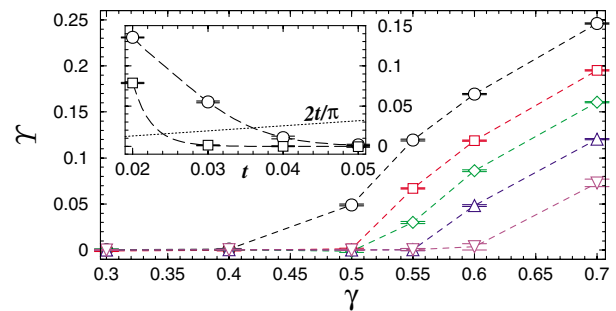


FIG. 4 (color online). Finite-size data ($L = 24$) for Y vs γ , at $t = 0.05$ and $g = 10$, for different values of P as in Fig. 3. Inset: $Y(t)$ for $\gamma = 0.55$ (circles) and $\gamma = 0.50$ (squares) for $L = 12$ and $P = 201$. The straight dotted line in the inset marks the universal-jump value $2t/\pi$.

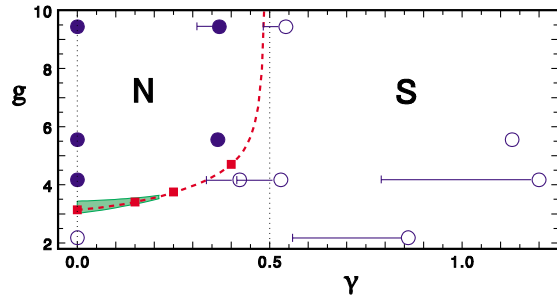


FIG. 5 (color online). Zero- t phase diagram. Squares: estimates of g_c from the data reported in Fig. 1. The dashed line extrapolates them to the expected behavior of $g_c(\gamma)$. Full and open circles: N and S phases, respectively, as observed experimentally [9]. The reentrant behavior occurs in the shadowed region.

of Y , signaling the proximity of the BKT critical line, shows up at $\gamma \approx 0.6$: as t is still finite, this value is only an upper bound for γ_c . Indeed, as shown in the inset, the transition occurs at low t also for $\gamma = 0.5$. Our results are therefore consistent with $\gamma_c = 1/2$, in agreement with early predictions [13–15]. In addition, the reentrance displayed at $\gamma = 0$ disappears well before $\gamma_c = 1/2$, so there is no evident connection between the two phenomena.

The quantum phase transition occurs at $g = g_c(\gamma)$ where the critical temperature $t_c(g, \gamma)$ vanishes: assuming that $\gamma_c = 1/2$ and using the data reported in Fig. 1 to estimate g_c for some values of γ , we can draw the line of quantum critical points $g_c(\gamma)$ that separates the S and N phase in the (γ, g) plane. Figure 5 evidences that the resulting zero- t phase diagram is in remarkable agreement with the experimental findings by Takahide *et al.* [9].

In conclusion, we have obtained the quantitative phase diagram of a resistively shunted 2D Josephson junction array. The reentrant low- T normal phase persists in a small but *finite* range of values of $\gamma \lesssim 0.2$ (i.e., $R_S \gtrsim 32$ k Ω) and $3.2 \lesssim g \lesssim 3.5$. This explains why the reentrance was not detected in the shunted JJA samples of Ref. [9], whose resistances $R_S \lesssim 18$ k Ω and quantum coupling values ($g = 2.2, 4.2, 5.5$, and 9.4) lie outside the above range. For $\gamma > \gamma_c = 1/2$ we observe the SN transition at finite t for very large coupling, thus validating the prediction that above γ_c the S phase is always stabilized. The reentrance is the most dramatic signature of the strong nonlinear quantum fluctuations characterizing the quantum critical region. Our results point out that the latter exists not only at $T = 0$ and $\gamma = 0$, but also at finite temperature and dissipation. Dissipation turns out to be a fundamental ingredient for future investigations since it allows one to tune (both in theory and in experiment) the system in and out of quantum criticality.

We thank J. V. José and Y. Takahide for fruitful correspondence. V.T. acknowledges the hospitality at the “Abdus Salam” ICTP-Trieste. This work has been supported by the COFIN2002-MIUR fund, and by EU-SQUBIT2 IST-2001-390083 (A. F.).

- [1] A. O. Caldeira and A. J. Leggett, *Ann. Phys. (N.Y.)* **149**, 374 (1983).
- [2] G. Schön and A. D. Zaikin, *Phys. Rep.* **198**, 237 (1990).
- [3] R. Fazio and H. S. J. van der Zant, *Phys. Rep.* **355**, 235 (2001).
- [4] Y. Makhlin, G. Schön, and A. Shnirman, *Rev. Mod. Phys.* **73**, 357 (2001).
- [5] B. Abeles, *Phys. Rev. B* **15**, 2828 (1977).
- [6] S. L. Sondhi, S. M. Girvin, J. P. Carini, and D. Shahar, *Rev. Mod. Phys.* **69**, 315 (1997).
- [7] H. S. J. van der Zant, W. J. Elion, L. J. Geerligs, and J. E. Mooij, *Phys. Rev. B* **54**, 10081 (1996).
- [8] A. J. Rimberg, T. R. Ho, Ç. Kurdak, J. Clarke, K. L. Campman, and A. C. Gossard, *Phys. Rev. Lett.* **78**, 2632 (1997).
- [9] Y. Takahide, R. Yagi, A. Kanda, Y. Ootuka, and S. I. Kobayashi, *Phys. Rev. Lett.* **85**, 1974 (2000).
- [10] B. J. Kim and M. Y. Choi, *Phys. Rev. B* **52**, 3624 (1995).
- [11] S. V. Panyukov and A. D. Zaikin, *J. Low Temp. Phys.* **75**, 361 (1989).
- [12] E. Šimánek and R. Brown, *Phys. Rev. B* **34**, R3495 (1986).
- [13] S. Chakravarty, G. L. Ingold, S. Kivelson, and A. Luther, *Phys. Rev. Lett.* **56**, 2303 (1986).
- [14] M. P. A. Fisher, *Phys. Rev. B* **36**, 1917 (1987).
- [15] S. Chakravarty, G. L. Ingold, S. Kivelson, and G. Zimanyi, *Phys. Rev. B* **37**, 3283 (1988).
- [16] J. Choi and J. V. José, *Phys. Rev. Lett.* **62**, 1904 (1989).
- [17] L. Capriotti, A. Cuccoli, A. Fubini, V. Tognetti, and R. Vaia, *Phys. Rev. Lett.* **91**, 247004 (2003).
- [18] V. L. Berezinskii, *Zh. Eksp. Teor. Fiz.* **59**, 907 (1970) [*Sov. Phys. JETP* **32**, 493 (1971)]; J. M. Kosterlitz and D. J. Thouless, *J. Phys. C* **6**, 1181 (1973).
- [19] P. Olsson, *Phys. Rev. Lett.* **73**, 3339 (1994); M. Hasenbusch and K. Pinn, *J. Phys. A* **30**, 63 (1997); S. G. Chung, *Phys. Rev. B* **60**, 11761 (1999).
- [20] A. Cuccoli, A. Fubini, V. Tognetti, and R. Vaia, *Phys. Rev. B* **61**, 11289 (2000).
- [21] C. Rojas and J. V. José, *Phys. Rev. B* **54**, 12361 (1996); A. I. Belousov and Yu. E. Lozovik, *Solid State Commun.* **100**, 421 (1996).
- [22] K. B. Efetov, *Zh. Eksp. Teor. Fiz.* **78**, 2017 (1980) [*Sov. Phys. JETP* **51**, 1015 (1980)]; E. Šimánek, *Phys. Rev. B* **32**, R500 (1985); J. V. José, *Phys. Rev. B* **29**, R2836 (1984); E. Granato and M. A. Continentino, *Phys. Rev. B* **48**, 15977 (1993); G. Grignani, A. Mattoni, P. Sodano, and A. Trombettoni, *Phys. Rev. B* **61**, 11676 (2000).
- [23] L. Capriotti, A. Cuccoli, A. Fubini, V. Tognetti, and R. Vaia, *Europhys. Lett.* **58**, 155 (2002); *Phys. Status Solidi B* **237**, 23 (2003).
- [24] U. Weiss, *Quantum Dissipative Systems* (World Scientific, Singapore, 1999).
- [25] F. R. Brown and T. J. Woch, *Phys. Rev. Lett.* **58**, 2394 (1987).
- [26] P. Werner and M. Troyer, *cond-mat/0409664*.
- [27] J. D. Doll, R. D. Coalson, and D. L. Freeman, *Phys. Rev. Lett.* **55**, 1 (1985).
- [28] C. P. Herrero and A. D. Zaikin, *Phys. Rev. B* **65**, 104516 (2002).